




# Study on the magnetic property of Fe–Si–B amorphous magnetic powder core coated with Al<sub>2</sub>O<sub>3</sub>/phosphoric acid–Al<sub>2</sub>O<sub>3</sub> double layer

Yong Zhu<sup>1</sup> , Cong Zhang<sup>1</sup>, Xiansong Liu, Xucai Kan<sup>1,\*</sup>, Shuangjiu Feng, Qingrong Lv, and Wei Sun<sup>2</sup>

<sup>1</sup>Engineering Technology Research Center of Magnetic Materials, Anhui Province, School of Materials Science and Engineering, Anhui University, Hefei 230601, People's Republic of China

<sup>2</sup>BGRIMM Technology Group Co. LTD, Beijing 100160, People's Republic of China

Received: 6 November 2022

Accepted: 19 December 2022

Published online:  
25 January 2023

© The Author(s), under exclusive licence to Springer Science+Business Media, LLC, part of Springer Nature 2023

## ABSTRACT

To study the magnetic loss of electronic devices in high-frequency applications, Fe–Si–B magnetic powder cores coated with Al<sub>2</sub>O<sub>3</sub> or phosphoric acid–alumina composite coating were prepared. In this paper, the effects of nano-Al<sub>2</sub>O<sub>3</sub> powders and phosphoric acid with different contents on magnetic properties such as magnetic loss and permeability of magnetic materials were investigated. In addition, three kinds of amorphous Fe–Si–B powders ( $D_{50} = 21.78 \mu\text{m}$ ,  $11.59 \mu\text{m}$ ,  $5.554 \mu\text{m}$ ) were mixed to find the best particle size ratio. The results show that the coating of mixture of 0.8 wt% phosphoric acid and 0.2 wt% Al<sub>2</sub>O<sub>3</sub> achieves excellent magnetic properties ( $\mu' = 22.34$ ;  $P_{\text{cv}} = 205.4 \text{ mW/cm}^3$  measured at 1000 kHz, 20 mT) with a particle size ratio of 2:6:2.

## 1 Introduction

Fe-based amorphous magnetic powder composites (SMCs) have attracted wide attention of researchers because of their low cost [1], high permeability [2], high saturation magnetization [3], especially the low eddy current loss of high frequency [4]. In the preparation process of magnetic powder core, insulating coating is an effective method to reduce eddy current loss. The surface of magnetic powder is coated with an insulating material which can block the direct contact between magnetic powder particles at high frequency, thus reducing the eddy current

loss between particles. Commonly used coating agents can be divided into organic coating agents and inorganic coating agents. Organic coating agents such as epoxy resin [5] and phenolic resin [6] have been widely used because of their excellent adhesion, but the low temperature stability of organic compounds limits their application range. Therefore, high-temperature resistant inorganic coating agents, such as Al<sub>2</sub>O<sub>3</sub> [7], SiO<sub>2</sub> [4, 8] and ZrO<sub>2</sub> [9], have been used in the preparation process of partial high temperature annealing. Furthermore, passivation by phosphoric acid [10] and direct addition of carbonyl iron [7, 10] or Ni–Zn [11, 12] ferrite with high magnetic

Address correspondence to E-mail: kanxucai@ahu.edu.cn

permeability are also hot spots of current research. Therefore, SMCs with low magnetic loss can be obtained using one or more inorganic coating agents.

Besides the influence of the coating material on magnetic powder loss, the original particle size of the material also affects the final molding density and the properties of the sample after annealing [13, 14]. With the increase of the particle size of magnetic powder, the permeability between powder increases, while SMCs with the same composition and small particle size have better stability and lower high frequency magnetic loss [15–17].

Due to the above characteristics, amorphous magnetic powders are widely used in magnetic powder cores, inductive devices, microwave absorbing materials [18, 19] and other fields, and has high research value. At present, although there have been studies on adding phosphoric acid [10] or  $\text{Al}_2\text{O}_3$  [7] separately in the process of preparing amorphous magnetic powder cores, generally only one of them is involved and the experiment on particle size distribution is rarely mentioned, which leads to imperfect experimental results. In this experiment,  $\text{Al}_2\text{O}_3$  and phosphoric acid–alumina double-layer coating agents were added to prepare magnetic powder cores, respectively. By comparing the coating results of single layer and double layer, the best additive amount of comprehensive performance could be found. Phosphoric acid and  $\text{Al}_2\text{O}_3$  were selected because of their low cost and good coating effect. This is why they are widely used in industrial production. There are many holes in phosphate on the surface of the powder passivated by phosphoric acid, which is beneficial to the addition of  $\text{Al}_2\text{O}_3$ . In addition, to study the influence of powder particle size and its ratio on magnetic powder core, three kinds of Fe–Si–B powders with different particle sizes were mixed in a certain proportion, and the influence of particle size ratio on the magnetic properties of the samples was studied.

## 2 Experimental details

The gas atomized spherical powders of Fe–Si–B (AMP-2, Tiz-Advanced Alloy Technology Co., Ltd, Fujian province, China) with three different particle sizes (X1:  $D_{50} = 21.78 \mu\text{m}$ ; X2:  $D_{50} = 11.59 \mu\text{m}$ ; X3:  $D_{50} = 5.554 \mu\text{m}$ ) were used in this experiment. The specific chemical composition and laser particle size

distribution are listed in Table 1. Besides, nanometer  $\text{Al}_2\text{O}_3$  powders with a particle size of 200 nm were also used in the experiment. The overall schematic diagram of the experiment is shown in Fig. 1. First, 0.2 wt%, 0.4 wt%, 0.6 wt%, 0.8 wt%, 1.0 wt%, 1.2 wt% and 1.5 wt% of alumina powders were added to 20 g X1 powder respectively and mixed thoroughly for 5 min. Then a certain amount of silicone resin dissolved in ethanol was added to enhance cohesiveness. After stirring for 10 min and drying at low temperature, the composites were evenly mixed with 0.5 wt% zinc stearate and pressed into a magnetic ring (outer diameter = 14.00 mm; inner diameter = 7.90 mm; thickness = 3.50 mm). At last, under the protection of nitrogen atmosphere, the finished ring was got after annealing at 480 °C for 1 h to eliminate the internal stress.

The process of double coating was similar to the above experiment, but before adding  $\text{Al}_2\text{O}_3$ , the amorphous powders needed to be passivated by adding phosphoric acid dissolved in absolute ethanol at 55 °C, and then nano-alumina powders were added after stirring and drying. The specific amount of phosphoric acid and  $\text{Al}_2\text{O}_3$  depended on the previous experimental results. Similarly, 1 wt% of silicone resin dissolved in ethanol was added, and after stirring for 10 min and drying, the composites were evenly mixed with 0.5 wt% zinc stearate and pressed into a magnetic ring. Finally, the magnetic ring was placed in nitrogen atmosphere and annealed at 480 °C for 1 h to obtain the final product.

The phase spectrum of amorphous magnetic cores was examined by X-ray diffraction (XRD, SmartLab) with  $\text{Cu K}\alpha$  radiation. The surface morphology of the sample was characterized by the scanning electron microscopy (SEM) model on an electron beam lithography system (EBL, Zeiss SIGMA500). Last, the magnetic properties like permeability and static hysteresis loop of the sample were measured by a B-H/ $\mu$  analyzer (SY-8258).

## 3 Results and discussion

### 3.1 $\text{Al}_2\text{O}_3$ insulation coating only

Firstly, the effect of  $\text{Al}_2\text{O}_3$  on the high frequency magnetic loss of the sample is studied. Figure 2 shows the curve of magnetic loss of magnetic powder coated different contents of  $\text{Al}_2\text{O}_3$  with frequency.

**Table 1** Chemical composition and laser particle size distribution of Fe–Si–B powder

AMP-2	Chemical composition						Laser particle size distribution ( $\mu\text{m}$ )		
	Item	Si	B	Fe	O	C	$D_{10}$	$D_{50}$	$D_{90}$
X1	Results (wt%)	3.0–6.0	3.0–6.0	Balance	0.2102	0.5403	8.125	21.78	54.02
X2		3.0–6.0	3.0–6.0	Balance	0.2511	0.5193	4.358	11.59	28.54
X3		3.0–6.0	3.0–6.0	Balance	0.4388	0.5439	2.323	5.554	10.96

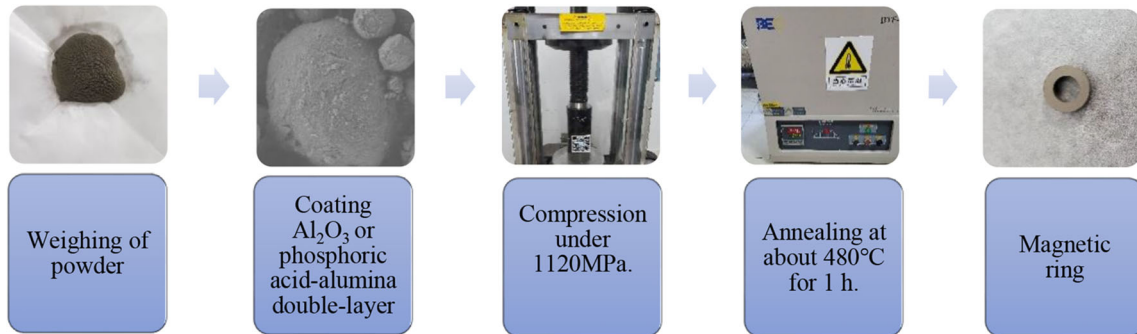


**Fig. 1** The overall schematic diagram of the experiment

Obviously, with the increase of frequency, the loss of magnetic rings rises rapidly. The raw material of X1 powder has the biggest loss of  $806 \text{ mW/cm}^3$ , nevertheless, rings coated with 1.0 wt%  $\text{Al}_2\text{O}_3$  only own  $532.7 \text{ mW/cm}^3$  measured at 1000 Hz, with a decrease of 33.9%. Adding more than 1.0 wt%  $\text{Al}_2\text{O}_3$  will not further reduce the loss, on the contrary, more  $\text{Al}_2\text{O}_3$  coating will increase the loss of the magnetic ring.

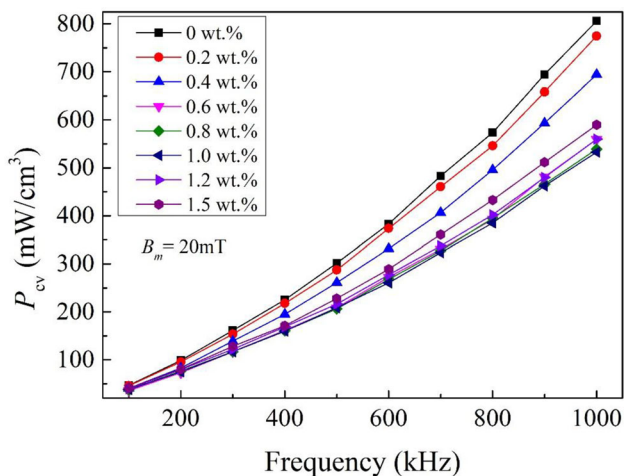


**Fig. 2** Magnetic loss of magnetic powder coated different contents of  $\text{Al}_2\text{O}_3$  varies with frequency at a magnetic flux density of 20 mT

Similarly, the permeability of magnetic rings is tested and showed in Fig. 3. The real part of permeability decreases from 26.01 at 0 wt% to 20.96 at 1.5 wt% while the imaginary part of permeability also falls distinctly. The decrease in the former is largely due to an increase in nonmagnetic materials  $\text{Al}_2\text{O}_3$ . However, regardless of the content, the true permeability of the sample decreases only slightly (less than 1%) when the frequency increases from 100 kHz to 1 MHz, demonstrating the excellent frequency stability of the magnetic ring. At the same situation, the imaginary part of permeability increases constantly with frequency. It is very small compared to the true permeability, only about 1–2% of latter.

### 3.2 Coated with phosphoric acid–alumina double layer

Based on the results of the above experiment, 0.8 wt% and 1.0 wt% are selected as the total contents of the double layer of phosphoric acid–alumina. Figure 4 shows the variation curves of magnetic loss of samples with frequency in two cases. Compared with the case of  $\text{Al}_2\text{O}_3$  coating only, the magnetic loss of the double-coated magnetic ring at high frequency is obviously reduced. In these two cases, the best magnetic loss properties are 0.8 wt% phosphoric acid

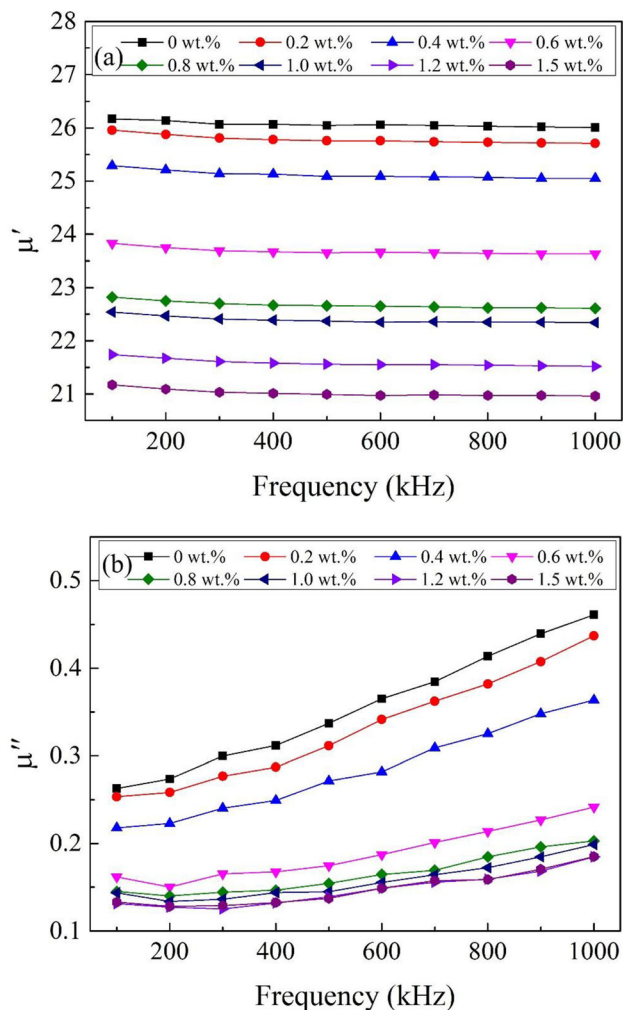


**Fig. 3** The real (a) and imaginary parts (b) of permeability of Fe-Si-B amorphous powder coated with Al<sub>2</sub>O<sub>3</sub> with different mass fraction

coating, 0.8 wt% phosphoric acid and 0.2 wt% Al<sub>2</sub>O<sub>3</sub> composite coating, respectively. Under the magnetic flux density of 20 mT and frequency of 1 MHz, their magnetic losses are 427.3 mW/cm<sup>3</sup> and 406 mW/cm<sup>3</sup>, respectively, which are reduced by 47.0% and 49.6% compared with the original powder. As shown in the Fig. 4, the magnetic loss performance of the magnetic ring coated with phosphoric acid is better than that of the magnetic ring coated with Al<sub>2</sub>O<sub>3</sub>, which may be caused by the inevitable oxidation of the sample surface during the preparation process. However, the phosphoric acid coating formed a dense passivation layer on the sample surface in the first step, which effectively preventing the oxidation of air and retaining good magnetism.

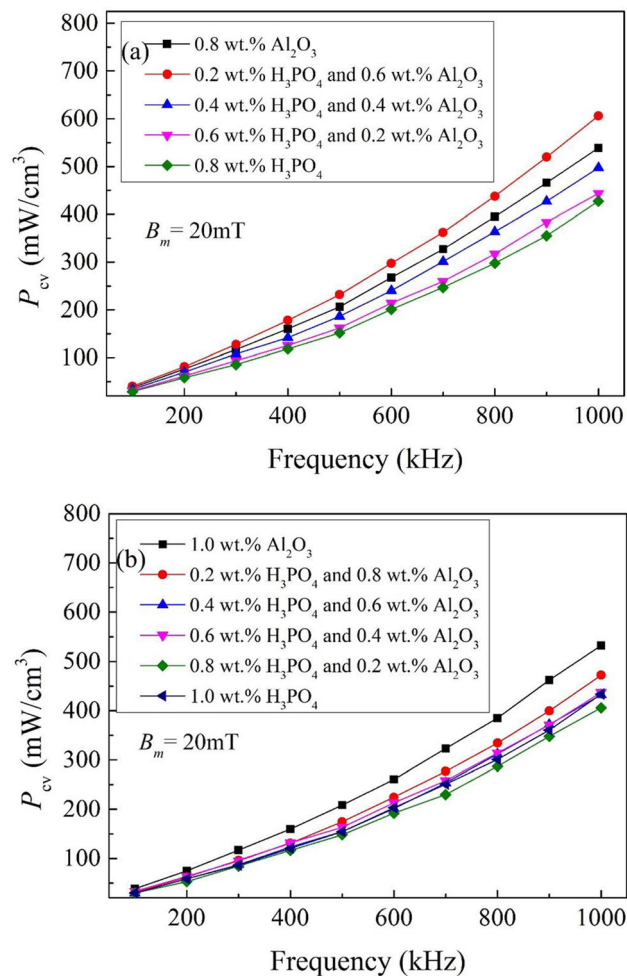


**Fig. 4** The change of magnetic loss with frequency of magnetic ring with flux density of 20 mT and total content of a 0.8 wt%, and b 1.0 wt%

Likewise, the magnetic permeability of magnetic ring is also studied as another important magnetic performance index in Fig. 5. In Fig. 5a, c, although the content of total nonmagnetic substances added in the two cases is constant, the permeability is different with different addition ratios. Compare Figs. 4 and 5, higher magnetic loss usually means higher magnetic permeability of the sample. The imaginary part of the permeability of the sample is shown in Fig. 5b and d, respectively. Like the single coating, their values are small, which indicates an excellent quality factor of the sample. According to the results of the above experiments, the magnetic rings coated with 0.6–0.2 wt% and 0.8–0.2 wt% phosphoric acid–alumina have the best comprehensive magnetic properties.

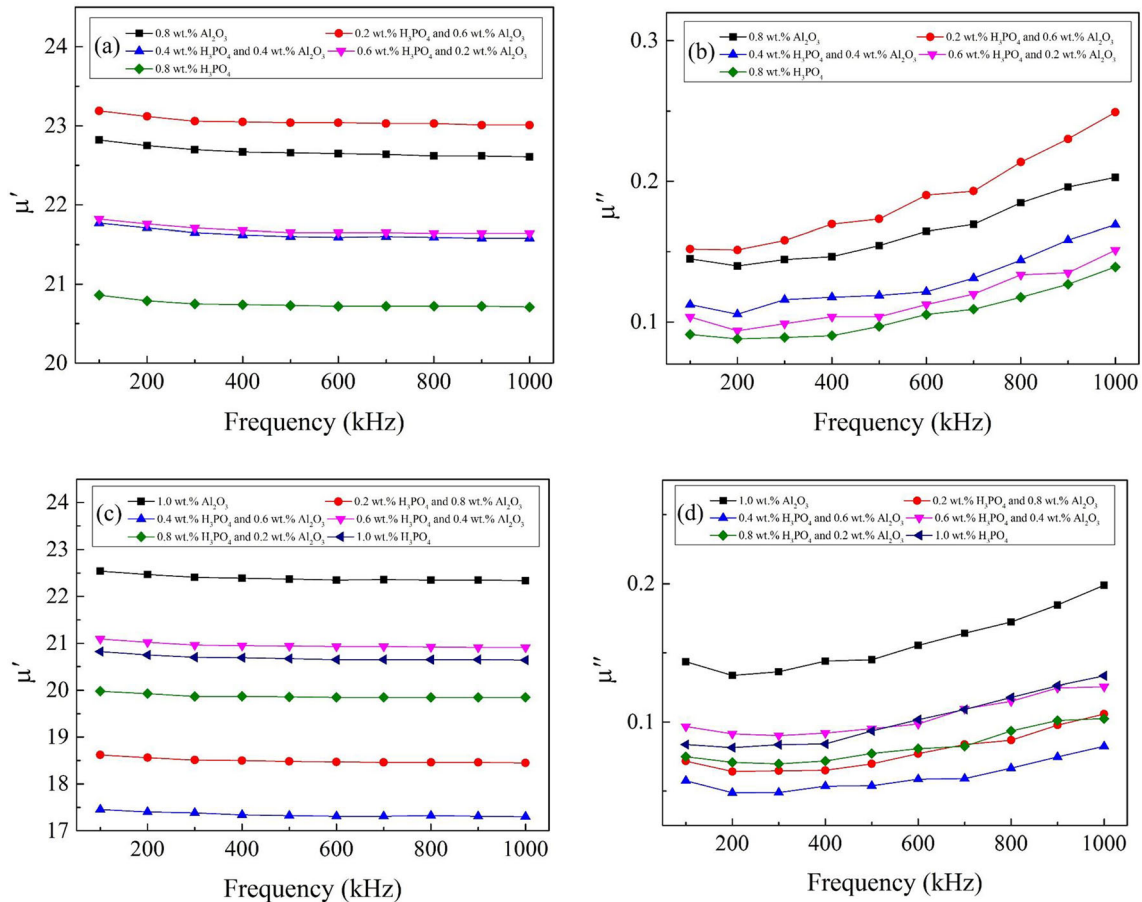


**Fig. 5** The real (a) and imaginary parts (b) of permeability of Fe-Si-B amorphous powder coated with phosphoric acid-alumina double layer of a total content of 0.8 wt%; the real (c) and

imaginary parts (d) of permeability of Fe-Si-B amorphous powder coated with phosphoric acid-alumina double layer of a total content of 1.0 wt%

### 3.3 Effect of particle size distribution on magnetic properties of samples

In this experiment, the purpose of using atomized spherical powder is to make it easier to study the maximum density of spheres. Figure 6a-c show the electron microscopy pictures of three powders with different particle size. It can be clearly found in the figure that although the three powders are different in size, they are all spherical with smooth surface, which is also the basis of follow-up experiments. The coating conditions of phosphoric acid alone, double coating and mixed particle size are shown in Fig. 6d, e, and f respectively. Compared with the original powder, the surface of the sample coated with phosphoric acid is obviously rough, which is due to the passivation reaction between phosphoric acid and iron powder, resulting in the formation of phosphate on the particle surface. In Fig. 6f, the uniform

distribution of spheres with different sizes also proves the feasibility of particle size distribution.

Figure 7 shows XRD pattern of raw materials powder with three different particle size after untreated and annealed at 480 °C for 1 h. It can be clearly found in the figure that the treatment temperature of 480 °C has little effect on the crystallization of amorphous powder, which indicates that the annealing temperature has no obvious damage to the cladding layer, and the effect of direct contact of powder on the magnetic properties of the sample is excluded.

Firstly, the raw powder is analyzed. Only 1.0 wt% silicone resin is added to increase the cohesiveness, and the three powders are pressed and molded. The data after annealing is shown in Table 2. The density is measured by Archimedes drainage method. With the decrease of the particle size of the powder, the magnetic loss of the sample is greatly reduced, but at

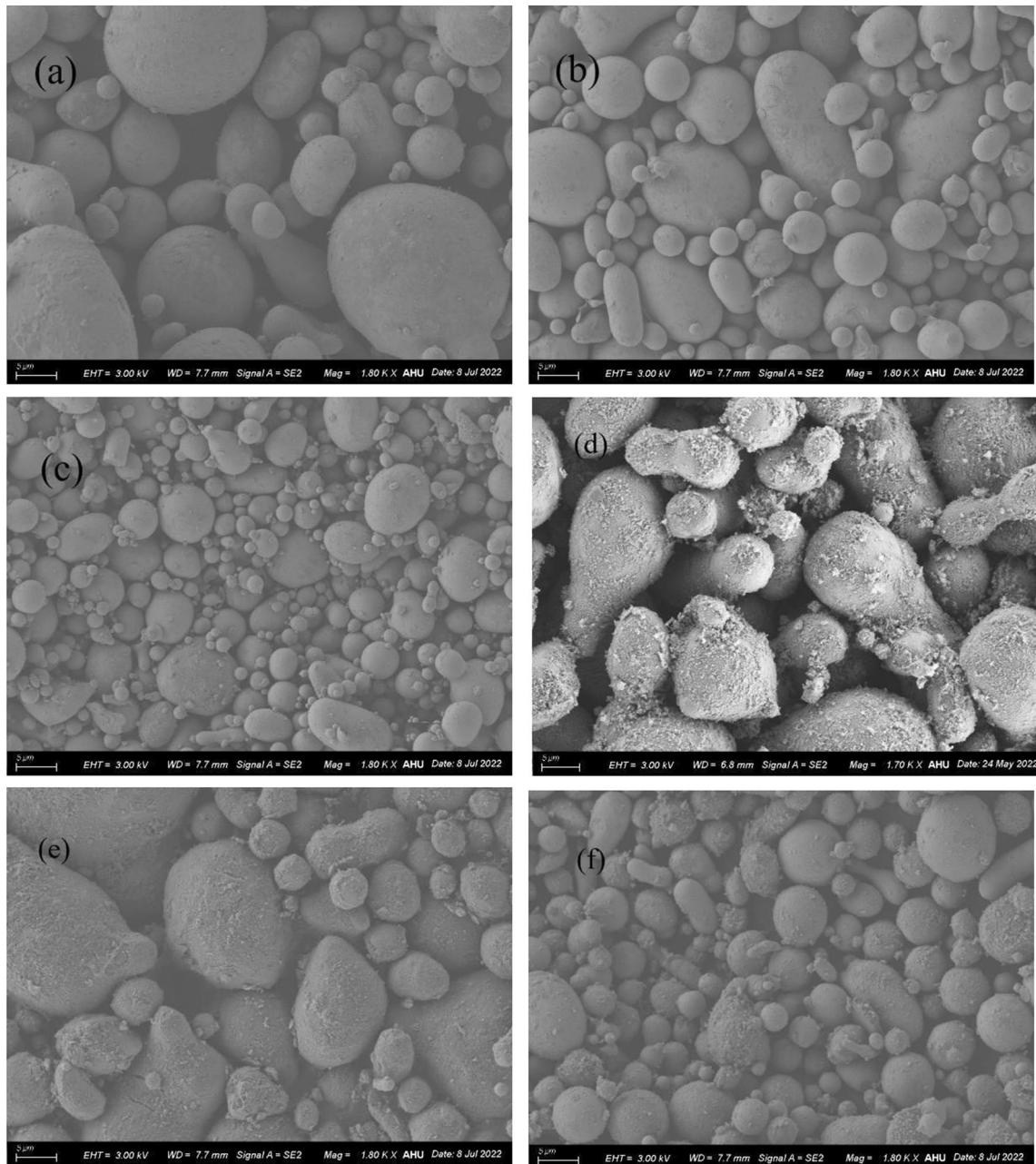


**Fig. 6** The electron microscopy pictures of **a** X1, **b** X2, **c** X3 amorphous powder, **d** X1 powder coated with 0.8 wt% phosphoric acid, **e** X1 powder coated with 0.8–0.2 wt% phosphoric acid–

alumina, and **f** the powder with ratio of 2:6:2 coated with 0.8–0.2 wt% phosphoric acid–alumina

the same time, the permeability is also decreased a lot. In order to get the desired sample, it is also the purpose of this experiment: to reduce the magnetic loss of the magnetic ring while keeping the permeability of the sample as much as possible. Therefore, samples mixed with these amorphous powders of different particle size are prepared. According to known research [20], 80% of the powder with large

particle size and 20% of the powder with small particle size can achieve the ideal bulk density and magnetic properties. Although some other research results on particle size distribution are somewhat different [21, 22], the scheme focusing on larger particle size powder is generally accepted. For this reason, the powder with the smallest particle size (X3)

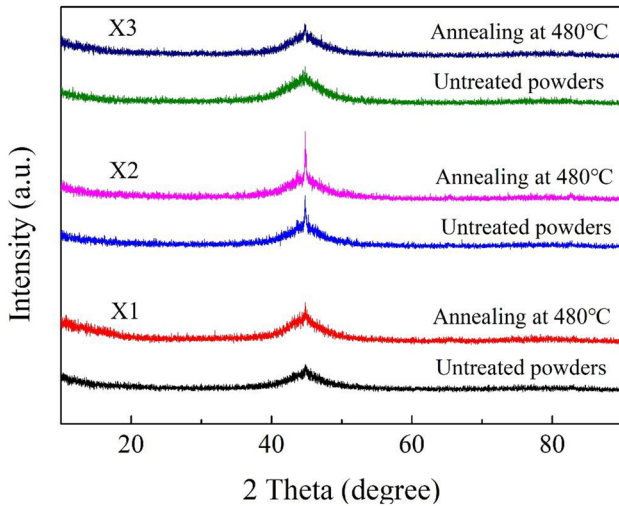


**Fig. 7** XRD spectrum of Fe-Si-B amorphous powder after untreated or annealed at 480 °C for 1 h

**Table 2** Magnetic properties of annealed amorphous powder at 1 MHz and 20 mT

Sample name	$P_{cv}$ (mW/cm <sup>3</sup> )	$\mu'$	Density (g/cm <sup>3</sup> )
X1	806.0	26.01	5.483
X2	278.8	22.70	5.545
X3	141.2	19.83	5.404

are added only 20%, and the other two larger powder (X1, X2) account for 80% of the total amount.

After repeating the above experimental steps, the magnetic properties of samples prepared with different particle size are shown in Fig. 8. The density measured by Archimedes drainage method is shown in Fig. 9. Compared with the original X1 powder, composite samples with powder of smaller particle have more ideal magnetic loss and nearly close true permeability. With the increase of the proportion of X1 powder and the decrease of the proportion of X2 powder, the magnetic loss of the sample decreases slightly at first, and then rises sharply. Accordingly, the permeability of the magnetic ring also presents the same trend. Before the ratio of X1 and X2 powder is the same, the increase of a large proportion of powder will lead to the deterioration of the magnetic properties of the samples. This may be related to the molding density of the sample [23]. As shown in Fig. 9, with the increase of the ratio of X1 powder, the density of magnetic powder core increases gradually, while before the ratio of 4:4:2, the density increases obviously. When the powder ratio reaches 3:5:2, the

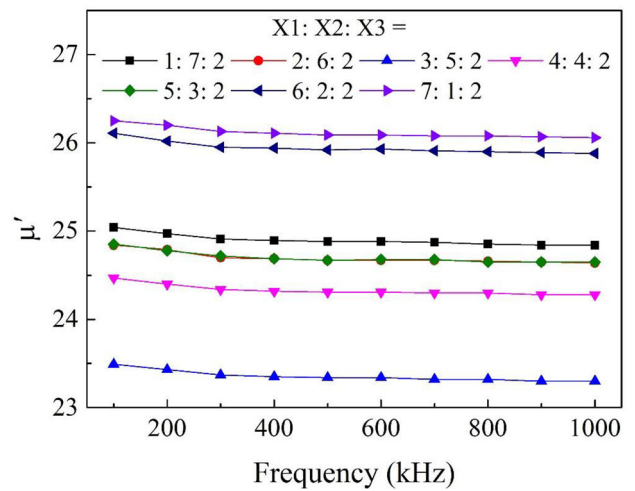
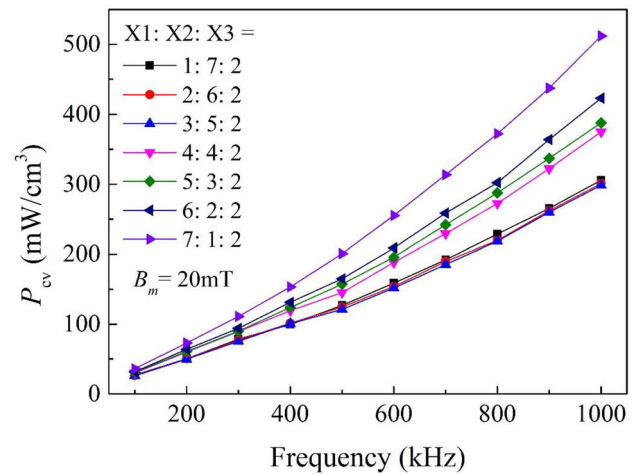


**Fig. 8** The variation curves of magnetic loss and true permeability with frequency of samples with different particle size

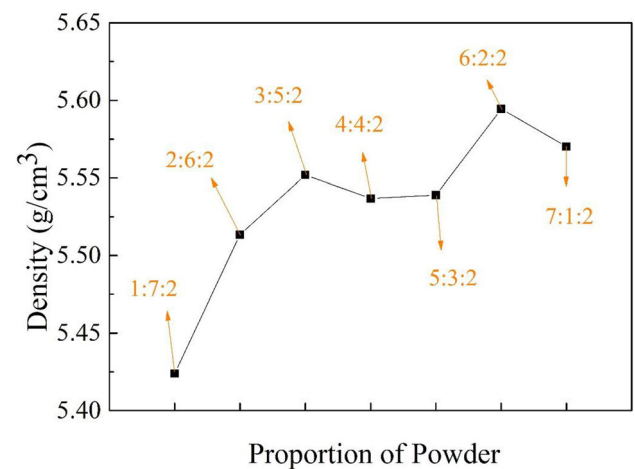


**Fig. 9** Density of magnetic cores with different proportion measured by Archimedes drainage method

density of the sample is 5.552 g/cm, 0.128 g/cm<sup>3</sup> lower than that of 1:7:2, which is due to the decrease of filling gaps between particles. At the same time, the sample which the powder ratio of 3:5:2 has the lowest magnetic loss ( $P_{cv} = 298.6 \text{ mW/cm}^3$  measured at 1000 kHz, 20 mT) and the lowest true permeability ( $\mu_e = 23.3$ ). However, this is not the limit.

In order to obtain better magnetic properties, the samples with powder ratio of 2:6:2 and 6:2:2 are selected for insulation coating, because these two samples have better comprehensive properties. The best scheme in the experiment of using the above-mentioned double-layer coating is adopted. The magnetic loss and true permeability image of the final powder core are shown in Fig. 10. It can be clearly seen in the figure that the magnetic loss of the sample with the ratio of 2:6:2 is lower than that of the sample with the ratio of 6:2:2, and the magnetic permeability of the double-layer coating decreases with the increase of phosphoric acid content, which proves the accuracy of the experiment. Among them, the loss of the double-layer coated sample made of powder with the ratio of 2:6:2 is 260.6 mW/cm<sup>3</sup> and 205.4 mW/cm<sup>3</sup>, respectively, which is 13.5% and 31.8% lower than that of the original powder ( $P_{cv} = 301.1 \text{ mW/cm}^3$ ) with the same ratio at 1000 kHz and 20 mT. Meanwhile, the magnetic loss of the double-layer coated powder core made of 6:2:2 powder is 365.7 mW/cm<sup>3</sup> and 333.5 mW/cm<sup>3</sup> respectively, which is 13.6% and 21.2% lower than that of the original powder ( $P_{cv} = 423.4 \text{ mW/cm}^3$ ) respectively. In terms of true permeability, the results of the four cases are close. Under the frequency field of 1000 kHz, the true permeability of the 2:6:2 sample is 22.88 and 22.34, respectively, which is 1.76 and 2.3 lower than that of the original powder, while the true permeability of the core made of two 6:2:2 powder is 22.77 and 22.72 respectively, which is 3.21 and 3.16 lower than that of the original powder. From the above analysis, it can be seen that the sample prepared by coating 0.8 wt% phosphoric acid and 0.2 wt% Al<sub>2</sub>O<sub>3</sub> with the particle size ratio of 2:6:2 has the best comprehensive magnetic properties ( $\mu' = 22.34$ ;  $P_{cv} = 205.4 \text{ mW/cm}^3$  measured at 1000 kHz, 20 mT).

### 3.4 Effect of silicone resin in process of coating

In this experiment, a certain amount of silicone resin was added as binder in the sample preparation

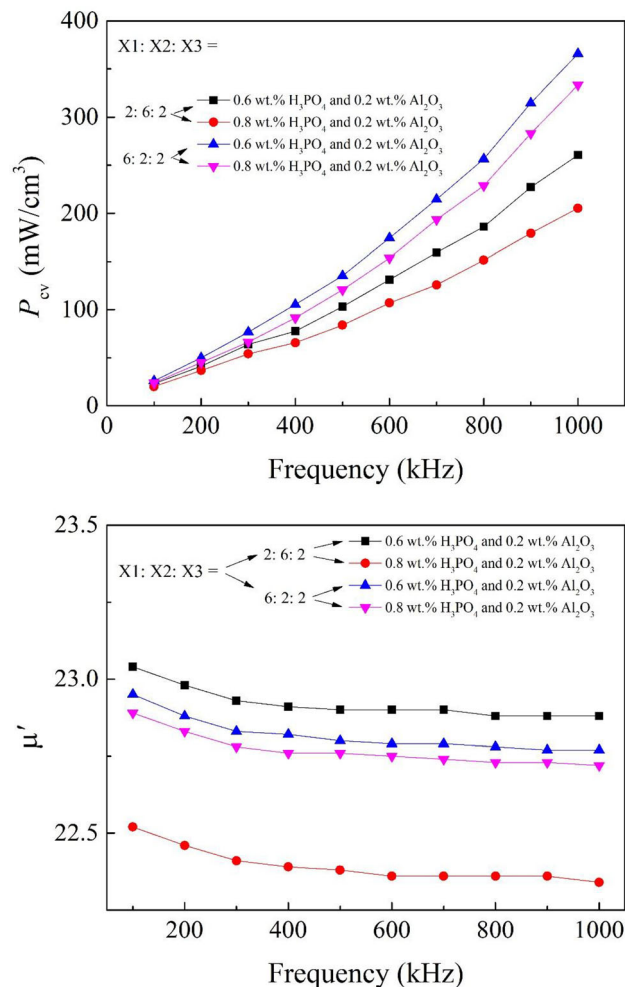


**Fig. 10** Magnetic loss and true permeability of Fe–Si–B magnetic powder core coated with phosphoric acid–alumina double layer with particle diameter ratio of 2:6:2 and 6:2:2

process to improve the cohesiveness of molding materials. Therefore, the magnetic ring coated with phosphoric acid with different content of silicone resin was analyzed for its possible influence on the coating layer. The results are shown in Table 3.

When the amount of silicone resin is less than 0.5 wt%, it is difficult to form the magnetic ring under laboratory pressure, so the experiment was carried out at about 1 wt%. It can be seen from Table 3 that the addition of silicone resin has little effect on the magnetic loss of phosphate coated powder at high and low frequency, and the loss of the sample with 1.5 wt% silicone resin is only 13.7% (1000 kHz) higher than that of 0.5 wt%. Meanwhile, with the increase of the additive amount, the true permeability of the sample first increases and then decreases, reaching the peak value (25.34) when the additive amount is



**Table 3** Magnetic properties of the X1 magnetic ring coated with 0.8 wt% phosphoric acid with different content of silicone resin

Silicone resin content (wt%)	$P_{cv}$ (mW/cm <sup>3</sup> )			$\mu'$ (1000 kHz)
	100 kHz	500 kHz	1000 kHz	
0.50	28.37	157.33	454.77	23.27
0.75	28.31	159.60	449.50	24.44
1.00	32.07	180.50	486.93	25.34
1.25	33.70	198.40	501.17	24.04
1.50	34.92	196.67	516.90	21.30

1.0 wt%, which is very close to the data of the original powder. Therefore, 1.0 wt% silicone resin is chosen in this experiment.

### 3.5 Study on loss separation of samples

According to Taghvaei’s study [24] of loss separation, the loss of SMCs ( $P_{cv}$ ) is composed of three parts: hysteresis loss ( $P_h$ ), eddy current loss ( $P_e$ ) and excess loss ( $P_r$ ). It can be explained in detail as the following equation.

$$P_{cv} = P_h + P_e + P_{exc} \tag{1}$$

The total energy loss ( $W_t$ ) can divide into three parts by dividing Eq. (1) by frequency factor. The results are as follows.

$$W_t = \frac{P_{cv}}{f} = \frac{P_h}{f} + \frac{P_e}{f} + \frac{P_{exc}}{f} = C_h + C_e f + C_{exc} \sqrt{f}, \tag{2}$$

where  $C_h$ ,  $C_e$ , and  $C_{exc}$  are loss coefficient respectively of three different loss energy.

According to the above analysis, the excess loss is caused by the compensation of the external magnetic field to the inhomogeneous internal counter-fields. In this experiment, the imaginary part of the permeability of the sample is very small (less than 1% of the real part), so the excess loss can be ignored. As for the hysteresis loss energy  $W_h$ , it can be reflected by the area of the static hysteresis loop, so the experimental loss separation can be achieved by fitting the  $B-H$  loop of the sample. Finally, eddy current loss is usually divided into inter-particle (it always exists between particles and is closely related to the degree of coating of the insulating material) loss and intra-particle (usually produced within particles, it is difficult to interfere with) loss, both have direct connection with the density and electric resistance, as Eqs. (3) and (4) present. Figure 11 shows the loss separation curve and specific loss of the magnetic

ring coated with different mass fractions of  $Al_2O_3$  at 0–500 kHz.

$$P_e^{Inter} = \frac{(pd_{eff}B_m)^2}{\beta\rho} f^2, \tag{3}$$

$$P_e^{Intra} = \frac{(pdB_m)^2}{20\rho} f^2, \tag{4}$$

where  $\beta$  is a variable that depends on the material itself and has to do with the shape and mass of the material,  $B_m$  the magnitude of magnetic induction,  $\rho$  the electric resistance,  $f$  the frequency,  $d_{eff}$  the effective distance between particles,  $d$  the particle size.

It can be seen from Fig. 11 that the hysteresis loss of the material increases with the addition of  $Al_2O_3$ , because the magnetic permeability of the material is reduced by the addition of nonmagnetic substances (Fig. 3). However, with the addition of alumina, the eddy current loss of the sample decreases first and then increases, and the peak value is 1.0 wt%. The decrease of eddy current loss is due to the insulation coating blocking the direct contact between particles, which greatly reduces the inter-particle loss, while

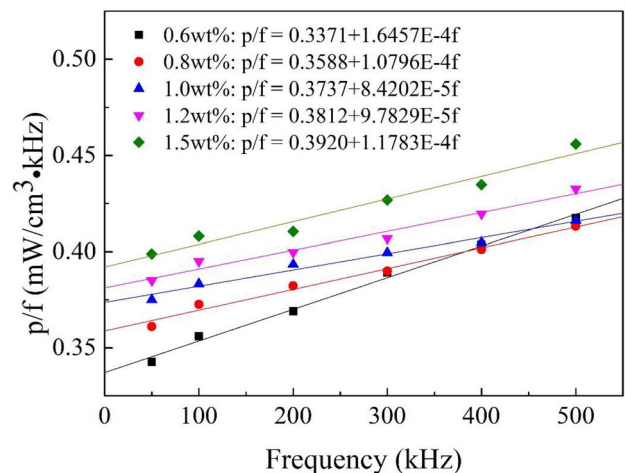


**Fig. 11** Loss of magnetic rings with different alumina coating amount per cycle

**Table 4** Comparative analysis of actual loss and theoretical loss at 1000 kHz, 20 mT

Al <sub>2</sub> O <sub>3</sub> content (wt%)	Actual loss (mW/cm <sup>3</sup> )	Theoretical loss (mW/cm <sup>3</sup> )	Difference (mW/cm <sup>3</sup> ) and proportion
0.6	559.50	501.67	57.83 (10.34%)
0.8	539.00	466.76	72.24 (13.40%)
1.0	532.70	457.90	74.80 (14.04%)
1.2	559.80	479.03	80.77 (14.42%)
1.5	589.90	509.83	80.07 (13.57%)

**Table 5** Loss separation of magnetic ring at 100 kHz and 500 kHz, respectively

Al <sub>2</sub> O <sub>3</sub> content (wt%)	Hysteresis loss (mW/cm <sup>3</sup> )		Eddy current loss (mW/cm <sup>3</sup> )	
	100 kHz	500 kHz	100 kHz	500 kHz
0.6	33.71	168.55	1.65	41.14
0.8	35.88	179.40	1.08	26.99
1.0	37.37	186.85	0.84	21.05
1.2	38.12	190.60	0.98	24.46
1.5	39.20	196.00	1.18	29.46

the abnormal rise after 1.0 wt% may be due to the excessive addition of alumina, which improves the brittleness of the sample, and the insulation layer is destroyed during pressing, and the inter-particle loss increases again.

The loss separation below 500 kHz as mentioned above, the fitted function is quite consistent with the data. However, when the frequency is above 500 kHz, the actual total loss value is larger than the result obtained by the formula. Detail value shows in Tables 4 and 5.

From the above data, the excess loss of the sample can't be ignored at the high frequency above 500 kHz, and it tends to increase with the increase of frequency. Meanwhile, in the frequency range that can keep a linear relationship, it can be clearly found that the proportion of eddy current loss increases rapidly with the frequency increasing. For example, the eddy current loss of the sample with 1.0 wt% Al<sub>2</sub>O<sub>3</sub> increased from 0.84 mW/cm<sup>3</sup> (2.2%) at 100 kHz to 21.05 mW/cm<sup>3</sup> (11.0%) at 500 kHz, but obviously the hysteresis loss still dominates in this frequency range.

## 4 Conclusion

In this paper, the magnetic properties of samples coated with alumina, double-layer coated with phosphoric acid–alumina and powder with different

particle sizes were analyzed, and the specific change reasons were studied by loss separation. Electron microscope image and pictures of *B–H* analyzer showed a dense coating layer was formed on the surface of the sample, and the sample coated with 0.8 wt% phosphoric acid and 0.2 wt% alumina had the best comprehensive magnetic properties ( $\mu' = 22.34$ ;  $P_{cv} = 205.4$  mW/cm<sup>3</sup> measured at 1000 kHz, 20 mT) with the particle size ratio of 2:6:2. Moreover, the loss separation results showed that when the particle size is small, the insulation coating had a weak effect on reducing eddy current loss of Fe–Si–B powder. Therefore, this study not only provided a feasible coating method for related research, but also served as a reference for future research on particle size ratio. Adjusting the particle size ratio may be a better choice for small particle size powder.

## Author contributions

YZ: Conceptualization, Formal analysis, Data curation, Writing—original draft, Visualization. CZ: Methodology, Validation. XL: Funding acquisition. XK: Resources, Writing—review and editing, Supervision. SF: Formal analysis, Investigation. QL: Project administration. WS: Funding acquisition.

## Funding

This work was supported by the National Key R&D Program of China (Grant No. 2021YFB3502400), the National Natural Science Foundation of China (No. 51872004), the Key Research and Development Plan of Anhui Province (Nos. 201904a05020038, 202003a05020051).

## Data availability

All data generated or analysed during this study are included in this published article.

## Declarations

**Competing interests** The authors have no competing interests to declare that are relevant to the content of this article.

## References

1. L. Zhang, D. Li, Z. Lu, C. Lu, T. Liu, F. Guo et al., Novel Fe-based amorphous magnetic powder cores with ultra-low core losses. *Sci. China Technol. Sci.* **53**(5), 1290–1293 (2010). <https://doi.org/10.1007/s11664-020-08607-8>
2. C. Chang, Y. Dong, M. Liu, H. Guo, Q. Xiao, Y. Zhang, Low core loss combined with high permeability for Fe-based amorphous powder cores produced by gas atomization powders. *J. Alloys Compd.* **766**, 959–963 (2018). <https://doi.org/10.1016/j.jallcom.2018.07.055>
3. Y. Han, F.L. Kong, F.F. Han, A. Inoue, S.L. Zhu, E. Shalaan et al., New Fe-based soft magnetic amorphous alloys with high saturation magnetization and good corrosion resistance for dust core application. *Intermetallics* **76**, 18–25 (2016). <https://doi.org/10.1016/j.intermet.2016.05.011>
4. X. Li, G. Lu, Z. Zhang, D. Ju, A. Makino, Bulk amorphous powder cores with low core loss by spark-plasma sintering Fe<sub>76</sub>Si<sub>9.6</sub>B<sub>8.4</sub>P<sub>6</sub> amorphous powder with small amounts of SiO<sub>2</sub>. *J. Alloys Compd.* **647**, 917–920 (2015). <https://doi.org/10.1016/j.jallcom.2015.05.139>
5. Y. Zhang, Y. Dong, L. Liu, L. Chang, B. Zhou, Q. Chi et al., High filling alumina/epoxy nanocomposite as coating layer for Fe-based amorphous powder cores with enhanced magnetic performance. *J. Mater. Sci. Mater. Electron.* **30**(16), 14869–14877 (2019). <https://doi.org/10.1007/s10854-019-01858-0>
6. M. Strečková, J. Fúzer, L. Kobera, J. Brus, M. Fáberová, R. Bureš et al., A comprehensive study of soft magnetic materials based on FeSi spheres and polymeric resin modified by silica nanorods. *Mater. Chem. Phys.* **147**(3), 649–660 (2014). <https://doi.org/10.1016/j.matchemphys.2014.06.004>
7. S. Choi, S. Lee, C.Y. Bon, K. Lee, S.J. Choi, S.-I. Yoo, Novel fabrication method for a high-performance soft-magnetic composite composed of alumina-coated Fe-based metal powder. *J. Electron. Mater.* **50**(2), 664–674 (2020). <https://doi.org/10.1007/s11664-020-08607-8>
8. K.-Y. Huang, Y.-Q. Dong, M. Liu, J.-H. Ren, S.-H. Lu, Z.-K. Zhao et al., Controllable SiO<sub>2</sub> coating layer of FeSiBPNb amorphous powder cores with excellent soft magnetic properties. *J. Iron Steel Res. Int.* **25**(6), 624–629 (2018). <https://doi.org/10.1007/s42243-018-0093-4>
9. K. Geng, Y. Xie, L. Yan, B. Yan, Fe–Si/ZrO<sub>2</sub> composites with core-shell structure and excellent magnetic properties prepared by mechanical milling and spark plasma sintering. *J. Alloys Compd.* **718**, 53–62 (2017). <https://doi.org/10.1016/j.jallcom.2017.05.114>
10. H.-I. Hsiang, L.-F. Fan, J.-J. Hung, Phosphoric acid addition effect on the microstructure and magnetic properties of iron-based soft magnetic composites. *J. Magn. Magn. Mater.* **447**, 1–8 (2018). <https://doi.org/10.1016/j.jmmm.2017.08.096>
11. J. Chang, T. Zhan, X. Peng, J. Li, Y. Yang, J. Xu et al., Improved permeability and core loss of amorphous FeSiB/Ni–Zn ferrite soft magnetic composites prepared in an external magnetic field. *J. Alloys Compd.* (2021). <https://doi.org/10.1016/j.jallcom.2021.161335>
12. L. Xiaolong, D. Yaqiang, L. Min, C. Chuntao, W. Xin-Min, New Fe-based amorphous soft magnetic composites with significant enhancement of magnetic properties by compositing with nano-(NiZn)Fe<sub>2</sub>O<sub>4</sub>. *J. Alloys Compd.* **696**, 1323–1328 (2017). <https://doi.org/10.1016/j.jallcom.2016.11.241>
13. R. Nowosielski, J.J. Wysłocki, I. Wnuk, P. Gramatyka, Nanocrystalline soft magnetic composite cores. *J. Mater. Process. Technol.* **175**(1–3), 324–329 (2006). <https://doi.org/10.1016/j.jmatprotec.2005.04.017>
14. D. Chen, K. Li, H. Yu, J. Zuo, X. Chen, B. Guo et al., Effects of secondary particle size distribution on the magnetic properties of carbonyl iron powder cores. *J. Magn. Magn. Mater.* (2020). <https://doi.org/10.1016/j.jmmm.2019.166062>
15. A.H. Taghvaei, H. Shokrollahi, M. Ghaffari, K. Janghorban, Influence of particle size and compaction pressure on the magnetic properties of iron-phenolic soft magnetic composites. *J. Phys. Chem. Solids.* **71**(1), 7–11 (2010). <https://doi.org/10.1016/j.jpcs.2009.08.008>
16. H.J. Woo, J.H. Ahn, C.P. Kim, D.H. Choi, S. Kim, B.W. Lee, Effect of the particle size classification of FeSiCrB

- amorphous soft magnetic composites to improve magnetic properties of power inductors. *J. Noncryst. Solids* (2022). <https://doi.org/10.1016/j.jnoncrsol.2021.121309>
17. J. Zhou, Y.F. Cui, H.S. Liu, W. Wang, K. Peng, Y.D. Xiao, Magnetic properties of  $\text{Fe}_{78.4}\text{Si}_{9.5}\text{B}_9\text{Cu}_{0.6}\text{Nb}_{2.5}$  nanocrystalline alloy powder cores. *J. Mater. Sci.* **46**(23), 7567–7572 (2011). <https://doi.org/10.1007/s10853-011-5731-1>
  18. H. Liang, L. Zhang, H. Wu, Exploration of twin-modified grain boundary engineering in metallic copper predominated electromagnetic wave absorber. *Small* **18**(38), e2203620 (2022). <https://doi.org/10.1002/sml.202203620>
  19. H. Liang, H. Xing, M. Qin, H. Wu, Bamboo-like short carbon fibers@ $\text{Fe}_3\text{O}_4$ @phenolic resin and honeycomb-like short carbon fibers@ $\text{Fe}_3\text{O}_4$ @FeO composites as high-performance electromagnetic wave absorbing materials. *Composites A* (2020). <https://doi.org/10.1016/j.compositesa.2020.105959>
  20. D. Grybos, J.S. Leszczynski, M. Kwiecień, C. Swieboda, P. Lasak, W. Pluta et al., Properties of Fe-based nanocrystalline magnetic powder cores (MPC) and structure of particle size distribution (PSD). *J. Electr. Eng.* **69**(2), 163–169 (2018). (<https://doi.org/10.2478/jee-2018-0020>)
  21. Y. Shi, Y. Zhang, Simulation of random packing of spherical particles with different size distributions. *Appl. Phys. A* **92**(3), 621–626 (2008). <https://doi.org/10.1007/s00339-008-4547-6>
  22. H.I. Hsiang, K.H. Chuang, W.H. Lee, FeSiCr alloy powder to carbonyl iron powder mixing ratio effects on the magnetic properties of the iron-based alloy powder cores prepared using screen printing. *Materials* (Basel) (2021). <https://doi.org/10.3390/ma14041034>
  23. Y. Chen, L. Zhang, H. Sun, F. Chen, P. Zhang, X. Qu et al., Enhanced magnetic properties of iron-based soft magnetic composites with phosphate–polyimide insulating layer. *J. Alloys Compd.* (2020). <https://doi.org/10.1016/j.jallcom.2019.152205>
  24. A.H. Taghvaei, H. Shokrollahi, K. Janghorban, H. Abiri, Eddy current and total power loss separation in the iron–phosphate–polyepoxy soft magnetic composites. *Mater. Des.* **30**(10), 3989–3995 (2009). <https://doi.org/10.1016/j.matdes.2009.05.026>

**Publisher's Note** Springer Nature remains neutral with regard to jurisdictional claims in published maps and institutional affiliations.

Springer Nature or its licensor (e.g. a society or other partner) holds exclusive rights to this article under a publishing agreement with the author(s) or other rightsholder(s); author self-archiving of the accepted manuscript version of this article is solely governed by the terms of such publishing agreement and applicable law.